# Saturated Backstepping-Based Tracking Control of a Quadrotor With Uncertain Vehicle Parameters and External Disturbances

Wei Xie, *Member, IEEE*, Weidong Zhang, *Senior Member, IEEE*, and Carlos Silvestre, *Senior Member, IEEE*

***Abstract*—Knowing the vehicle's parameters (e.g., mass, moment of inertia) in advance is not always possible in quadrotor control applications, especially if we use the quadrotor for cargo transportation. Uncertain cargo weight and size together with external disturbances may result in closed-loop performance degradation or even instability. In light of this problem, this letter proposes a saturated robust adaptive tracking controller for a quadrotor based on nonlinear Lyapunov-theory, where a set of estimation laws are designed to compensate for uncertain parameters and disturbances, achieving global uniformly ultimately boundedness (GUUB). Additionally, through the use of saturation functions, the designed thrust force is ensured to be bounded by a predefined value. Numerical simulation examples are presented and discussed to validate the effectiveness of the proposed solution. To further highlight the enhancements of the presented method, comparison results with an existing control strategy are provided and analyzed.**

***Index Terms*—Adaptive control, saturated control, trajectory tracking, quadrotor, disturbance rejection.**

Manuscript received August 21, 2021; revised October 24, 2021; accepted November 11, 2021. Date of publication November 23, 2021; date of current version December 2, 2021. This work was supported in part by the Key Research and Development Program of Guangdong under Grant 2020B1111010002; in part by the Key Research and Development Program of Hainan under Grant ZDYF2021GXJS041; in part by the National Natural Science Foundation of China under Grant U2141234; in part by the Macau Science and Technology, Development Fund under Grant FDCT/0031/2020/AFJ; in part by the University of Macau, Macau, China, under Project MYRG2020-00188-FST; and in part by the Fundação para a Ciência e a Tecnologia (FCT) through ISR LARSyS-FCT Project under Grant UIDB/50009/2020. Recommended by Senior Editor J.-F. Zhang. *(Corresponding author: Weidong Zhang.)*

Wei Xie is with the Department of Automation, Shanghai Jiao Tong University, Shanghai 200240, China (e-mail: weixie@sjtu.edu.cn).

Weidong Zhang is with the Department of Automation, Shanghai Jiao Tong University, Shanghai 200240, China, and also with the School of Information and Communication Engineering, Hainan University, Haikou 570228, Hainan, China (e-mail: wdzhang@sjtu.edu.cn).

Carlos Silvestre is with the Department of Electrical and Computer Engineering, Faculty of Science and Technology, University of Macau, Macau, China, on leave from the Instituto Superior Técnico, Universidade de Lisboa, 1049-001 Lisbon, Portugal (e-mail: csilvestre@um.edu.mo).

Digital Object Identifier 10.1109/LCSYS.2021.3129891

## I. Introduction

In RECENT years, unmanned aerial vehicles have shown many promising applications in both civilian and military fields, such as search, patrolling, mapping, load transportation, to name but a few [1]–[4]. Compared with fixed-wing aerial vehicles, rotorcraft have attracted more attention in academic research due to their distinguishing features, e.g., performing hover, vertical take-off and landing. Meantime, active research raises new and challenging problems, caused by their underactuated nature, uncertain vehicle parameters, external disturbances, etc., in accurate rotorcraft control.

Numerous control methods have been proposed in the literature to stabilize the rotorcraft along a desired smooth trajectory, such as PID [5], LQR [6], geometric control [7]–[9], backstepping-based techniques [10]–[12], sliding mode control [13]–[17], model predictive control [18], neural networks and fuzzy logic systems based control approaches [19]–[22], etc. Although the reported linear controllers [5], [6] have achieved good performance in tracking straight lines and trimming trajectories, both of them build on system linearization, resulting in the local stability. The above-mentioned nonlinear control methods, [7]–[14], [16]Ű[22], can overcome this limitation and attain larger regions of attraction. Moreover, it is worth pointing out that physical system constraint (e.g., actuation input constraint), which ubiquitously exist in practical applications, should also be addressed carefully. In our recent work [10], by introducing a few saturation functions in the controller design procedure, the resulting thrust force was ensured to be bounded with respect to position and linear velocity errors. In [18], the input constraint was guaranteed through solving an optimal control problem. However, neither [10] nor [18] considered uncertain vehicle parameters, i.e., they needed to assume that the system's mass and moment of inertia were known in advance, which is not always possible. For instance, in cargo transportation by rotorcraft, uncertain different weights and sizes of the cargo could lead to deteriorated flight performance if they (uncertainties) are not addressed properly.

Inspired by the above-mentioned works and discussions, the main contributions of this letter are summarized as follows.

1. Proposing a robust adaptive tracking controller for a class of second-order systems (SDSs) with uncertain system

parameter and external disturbance, guaranteeing that the control input is always bounded, and achieving global asymptotic stability;

2. Extending the proposed strategy for SDSs to solve the trajectory tracking problem with application to an underactuated quadrotor aerial vehicle, ensuring that
   - the quadrotor is globally driven to its desired smooth trajectory with arbitrarily small position error, attaining GUUB;
   - the generated thrust force is always saturated by a predefined value;
   - without needing to re-tune the control gains, the proposed approach is able to control a single quadrotor transporting cargo with uncertain weight and size, obtaining adaptive performance.

Rigorous stability proof and numerical simulation examples are presented to demonstrate the effectiveness of the proposed control strategy. Compared with the existing results, the improvements of the proposed method are described as follows. Different from [8], [12], [13], [15], [16], [19], [21], [23], the developed strategy is able to guarantee that the generated thrust force is always bounded by a predefined value which is demonstrated and illustrated by a rigorous theoretical proof and simulation results. Even though the input constraint can be ensured in [18], the vehicle's parameters are assumed to be known in advance. Improving on the saturated control method reported in [10] and the adaptive solution presented in [23], this letter provides a solution to deal with uncertain system mass, moment of inertial, and external disturbances simultaneously, attaining robust adaptive performance.

## II. Notation

In this letter, $\mathbb{R}^n$ denotes the n-dimensional Euclidean space. A function $\xi e : \mathbb{R} \mapsto \mathbb{R}^{n\times 1}$ is of class $\mathcal{C}^n$ if the derivatives $\xi', \xi'', \ldots, \xi^{(n)}$ exist and are continuous. Positive scalar set is denoted by $\mathbb{R}^+$. A differentiable saturation function is introduced as $\sigma(x) : \mathbb{R} \mapsto \mathbb{R}$, satisfying i) $|\sigma(x)| \leq \sigma_{\max}$, where $\sigma_{\max}$ is a known positive number; and, ii) $x\sigma(x) \geq 0$. For a vector $\mathbf{x} \in \mathbb{R}^{n\times 1}$, its saturation is represented by $\sigma(\mathbf{x}) = [\sigma(x_1), \ldots, \sigma(x_n)]^\mathsf{T}$. Unit vectors $\mathbf{u}_1, \mathbf{u}_2, \mathbf{u}_3$ are $\mathbf{u}_1 = [1, 0, 0]^\mathsf{T}, \mathbf{u}_2 = [0, 1, 0]^\mathsf{T}$ and $\mathbf{u}_3 = [0, 0, 1]^\mathsf{T}$, $\mathbf{I}_{n\times n} \in \mathbb{R}^{n\times n}$ denotes an identity matrix, $\mathbf{0}_{m\times n} \in \mathbb{R}^{m\times n}$ is a matrix whose entries are all zero, and $\mathbf{1}_{m\times n} \in \mathbb{R}^{m\times n}$ is a matrix whose entries are all one.

## III. Problem Formulation

This section first presents the quadrotor models, including kinematic and dynamic models. Then, the trajectory tracking problem is formally formulated.

### A. Quadrotor Model

We first introduce an inertial coordinate frame $\{I\}$ and a body-fixed coordinate frame $\{B\}$ attached to the quadrotor's center of mass. Then, the quadrotor's kinematic models can be rewritten as

$$\begin{aligned} \dot{\mathbf{p}} &= \mathbf{v} \\ \dot{\mathbf{R}} &= \mathbf{R}\mathbf{S}(\boldsymbol{\omega}) \end{aligned} \tag{1}$$

where $\mathbf{p} \in \mathbb{R}^{3\times 1}$ denotes the vehicle's position, while $\mathbf{R} \in \mathbb{R}^{3\times 3}$ represents the rotation matrix from $\{B\}$ to $\{I\}$. Correspondingly, the dynamic models can be expressed as

$$\begin{aligned} \dot{\mathbf{v}} &= -\Delta T\mathbf{R}\mathbf{u}_3 + g\mathbf{u}_3 + \mathbf{b}_v \\ \dot{\boldsymbol{\omega}} &= -\mathbf{J}^{-1}\mathbf{S}(\boldsymbol{\omega})\mathbf{J}\boldsymbol{\omega} + \mathbf{J}^{-1}\boldsymbol{\tau} \end{aligned} \tag{2}$$

where the map $\mathbf{S}(\cdot) : \mathbb{R}^3 \mapsto \mathbb{R}^{3\times 3}$ yields a skew-symmetric matrix that verifies $\mathbf{S}(\mathbf{x})\mathbf{y} = \mathbf{x} \times \mathbf{y}$ for any $\mathbf{x}$ and $\mathbf{y} \in \mathbb{R}^{3\times 1}$, and $\Delta = 1/m$. The linear velocity $\mathbf{v} \in \mathbb{R}^{3\times 1}$ is expressed in the $\{I\}$, while the angular velocity $\boldsymbol{\omega} \in \mathbb{R}^{3\times 1}$ is expressed in the $\{B\}$. The scalar $m$ and the diagonal matrix $\mathbf{J} = \mathrm{diag}(J_1, J_2, J_3)$ denote the quadrotor's mass and moment of inertia, respectively. The gravitational acceleration is denoted by $g \in \mathbb{R}$. The control inputs include the thrust force $T \in \mathbb{R}$ and torque $\boldsymbol{\tau} = [\tau_1, \tau_2, \tau_3]^\mathsf{T}$, and external disturbances $\mathbf{b}_v \in \mathbb{R}^{3\times 1}$ are expressed in the $\{I\}$.

*Assumption 1:* The quadrotor's mass, moment of inertia, and external disturbances are unknown, constant, and satisfy

$$m \in [m_{\min}, m_{\max}],\ \|\mathbf{J}\|_F \in [J_{\min}, J_{\max}],\ \|\mathbf{b}_v\| \leq \bar{b}_v$$

where $m_{\min}, m_{\max}, J_{\min}, J_{\max}, \bar{b}_v$ are known, positive numbers, with $m_{\max} > m_{\min}, J_{\max} > J_{\min}$.

### B. Problem Statement

Considering a smooth trajectory denoted by $\mathbf{p}_d(t) \in \mathbb{R}^{3\times 1}$, the objective is to design control laws for the thrust force $T$ and torque $\boldsymbol{\tau}$ such that the quadrotor's position $\mathbf{p}(t)$ can be globally driven to an arbitrarily small neighborhood of $\mathbf{p}_d(t)$, while the devised $T$ is guaranteed to be saturated by its physical upper bound $T_{\max}$.

*Definition 1 (Smooth Trajectory):* For any given trajectory $\mathbf{p}_d(t)$, if i) $\mathbf{p}_d(t)$ is a curve of at least class $\mathcal{C}^4$; and, ii) the time derivatives of $\mathbf{p}_d(t)$ are all bounded; then, $\mathbf{p}_d(t)$ is said to be smooth trajectory.

## IV. Controller Design

In this section, we start by designing an adaptive saturated controller for a general second-order system. Then, we apply the design idea to solve trajectory tracking problem with application to a quadrotor aerial vehicle.

### A. Second-Order System

Considering the following second-order system,

$$\ddot{x} = \lambda u + b$$

where $\lambda \in \mathbb{R}$ is a positive constant which is assumed to be uncertain but satisfies $\lambda \in [\lambda_{\min}, \lambda_{\max}]$, where $\lambda_{\min}, \lambda_{\max}$ are known positive numbers, $u \in \mathbb{R}$ is the control input, $b \in \mathbb{R}$ denotes the external constant disturbance which is unknown but satisfies $|b| \leq b_{\max}$, with $b_{\max} \in \mathbb{R}^+$. In the sequel, we will design an adaptive saturated controller for $u$ such that $x \in \mathbb{R}$ is able to track the desired smooth signal $x_d(t) \in \mathbb{R}$.

Defining the following two error terms as

$$z_a = x - x_d,\ z_b = \dot{x} - \dot{x}_d$$

and the Lyapunov candidate function

$$V_a = \frac{1}{2}z_b^2 + \frac{1}{\kappa_a}\int_0^{z_c} \sigma(s)ds$$

where $z_c = \kappa_a(z_a + \zeta z_b)$. Computing the time derivative of $V_a$, we have

$$\dot{V}_a = -W(z_b,\, z_c) + (z_b + \zeta\sigma(z_c))(\lambda u + b - \ddot{x}_d + \kappa_b\sigma(z_b + \zeta\sigma(z_c)) + \sigma(z_c)) \tag{3}$$

where $W(z_b,\, z_c) = \kappa_b(z_b + \zeta\sigma(z_c))\sigma(z_b + \zeta\sigma(z_c)) + \zeta\sigma(z_c)^2$, and $(\kappa_a,\, \kappa_b,\, \kappa_c) \in \mathbb{R}^+$.

Notice that $\lambda$, $b$ in (3) are unknown and cannot be explicitly included in the control laws. Therefore, we introduce their estimates denoted as $\hat{\lambda}$, $\hat{b}$, and the corresponding estimation errors are defined as

$$\tilde{\lambda} = \hat{\lambda} - \lambda,\ \tilde{b} = \hat{b} - b.$$

Defining the new Lyapunov candidate function by integrating $\tilde{\lambda}$, $\tilde{b}$ as

$$V_b = V_a + \frac{1}{\alpha}\int_0^{\tilde{\lambda}} (\hbar(\rho + \lambda) - \lambda)d\rho + \frac{1}{\beta}\int_0^{\tilde{b}} (\hbar(\rho + b) - b)d\rho \tag{4}$$

where $(\alpha,\, \beta) \in \mathbb{R}^+$ and the projection function $\hbar(\mu)$ is given as

$$\hbar(\mu) = \begin{cases} \mu_a + \epsilon\left(1 - \exp\left(\dfrac{\mu_a - \mu}{\epsilon}\right)\right), & \mu > \mu_a \\ \mu, & \mu \in [\mu_b,\, \mu_a] \\ \mu_b - \epsilon\left(1 - \exp\left(\dfrac{\mu - \mu_b}{\epsilon}\right)\right), & \mu < \mu_b \end{cases}$$

where $\mu_a > \mu_b$, $\epsilon \in \mathbb{R}^+$ can be chosen as small as possible. The time derivative of $V_b$ yields,

$$\begin{aligned}\dot{V}_b = {} & -W(z_b,\, z_c) + (z_b + \zeta\sigma(z_c))\Big(\hbar(\hat{\lambda})u + \hbar(\hat{b}) - \ddot{x}_d \\ & + \kappa_b\sigma(z_b + \zeta\sigma(z_c)) + \sigma(z_c)) + \Big(\hbar(\hat{\lambda}) - \lambda\Big) \\ & \times \Big(\dot{\hat{\lambda}}\alpha^{-1} - (z_b + \zeta\sigma(z_c))u\Big) + \Big(\hbar(\hat{b}) - b\Big) \\ & \times \Big(\dot{\hat{b}}\beta^{-1} - (z_b + \zeta\sigma(z_c))\Big).\end{aligned} \tag{5}$$

Choosing the control input for $u$ as

$$u = -\hbar^{-1}\Big(\hat{\lambda}\Big)\Big(\hbar(\hat{b}) - \ddot{x}_d + \kappa_b\sigma(z_b + \zeta\sigma(z_c)) + \sigma(z_c)\Big) \tag{6}$$

and the estimation laws for $\dot{\hat{\lambda}}$, $\dot{\hat{d}}$

$$\dot{\hat{\lambda}} = \alpha(z_b + \zeta\sigma(z_c))u,\ \dot{\hat{d}} = \beta(z_b + \zeta\sigma(z_c)). \tag{7}$$

Substituting (6) and (7) into (5), we have

$$\dot{V}_b = -\kappa_b(z_b + \zeta\sigma(z_c))\sigma(z_b + \zeta\sigma(z_c)) - \zeta\sigma(z_c)^2. \tag{8}$$

Notice that the designed input $u$ in (6) is well-defined since $\hbar(\hat{\lambda})$ is always positive.

*Remark 1:* The introduced projection function $\hbar(\mu)$ is of class $\mathcal{C}^1$ and guarantees that $\hbar(\mu) \in [\mu_b - \varepsilon,\, \mu_a + \varepsilon]$. The introduced terms $\int_0^{\tilde{\lambda}}(\hbar(\rho + \lambda) - \lambda)d\rho$, $\int_0^{\tilde{b}}(\hbar(\rho + b) - b)d\rho$ in (4) are positive [24], [25].

*Remark 2:* For a vector $\mathbf{x} = [x_1,\, \ldots,\, x_n]^\mathsf{T}$, its projection is denoted as $\hbar(\mathbf{x}) = [\hbar(x_1),\, \ldots,\, \hbar(x_n)]^\mathsf{T}$.

The main result is summarized in the following theorem.

*Theorem 1:* Considering the designed control input (6) and the estimation laws (7), the tracking errors $z_a$, $z_b$ are globally driven to zero, while the input satisfies $|u| \le \lambda_{\min}^{-1}(b_{\max} + a_{\max} + \kappa_b\sigma_{\max} + \sigma_{\max})$, where $|\ddot{x}_d| \le a_{\max}$, $a_{\max} \in \mathbb{R}^+$.

*Proof:* We start the proof by analyzing $\dot{V}_b$, defined in (8), from which we can conclude that $V_b$ is bounded. We further obtain that the second time derivative of $V_b$ is bounded as well, leading to the result that $\dot{V}_b$ is uniformly continuous. Trough the use of Barbalat's lemma, it can be concluded that $\dot{V}_b$ is driven to zero as time goes to infinity. As a consequence, $z_b$, $z_c$ converge to zero. Combing with $z_c = \kappa_z(z_a + \zeta z_b)$, we have that $z_a$ converges to zero as well. Considering the property of the introduced projection function $\mathsf{proj}(\mu)$, we have $|(\hbar(\hat{\lambda}))^{-1}| \le \lambda_{\min}^{-1}$, $|\hbar(\hat{b})| \le b_{\max}$, then, we get $|u| \le \lambda_{\min}^{-1}(b_{\max} + a_{\max} + \kappa_b\sigma_{\max} + \sigma_{\max})$. The proof is done. ■

*Remark 3:* The proposed solution in Section IV-A provides a general guideline on designing robust adaptive saturated controllers for a class of second-order systems, e.g., robotic manipulator, rotorcraft, rotorcraft-slung-load system, etc.

### B. Quadrotor System

Following the technique presented in Section IV-A, an adaptive saturated backstepping-based trajectory tracking controller is designed for a quadrotor aerial vehicle. Defining the position and velocity errors

$$\mathbf{z}_1 = \mathbf{p} - \mathbf{p}_d \tag{9}$$

$$\mathbf{z}_2 = \dot{\mathbf{z}}_1 - \mathbf{R}\boldsymbol{\delta} \tag{10}$$

with $\boldsymbol{\delta} = [0,\, 0,\, \delta]^\mathsf{T}$, $\delta \neq 0$. Computing the time derivative of $\mathbf{z}_1$ and $\mathbf{z}_2$, we have

$$\dot{\mathbf{z}}_1 = \mathbf{v} - \dot{\mathbf{p}}_d \tag{11}$$

$$\dot{\mathbf{z}}_2 = -\Delta T\mathbf{R}\mathbf{u}_3 + g\mathbf{u}_3 + \mathbf{b}_v - \ddot{\mathbf{p}}_d. \tag{12}$$

To stabilize (11) and (12), the thrust force $T$, and the estimation laws for $\widehat{\Delta}_1$ and $\widehat{\mathbf{b}}_{v_1}$ are chosen as

$$T = \hbar^{-1}(\widehat{\Delta})\mathbf{u}_3^\mathsf{T}\mathbf{n} \tag{13}$$

$$\dot{\widehat{\Delta}}_1 = -\gamma_1(\mathbf{z}_2 + \zeta\sigma(\mathbf{z}_0))^\mathsf{T}\mathbf{R}T\mathbf{u}_3 \tag{14}$$

$$\dot{\widehat{\mathbf{b}}}_{v_1} = \Lambda_1(\mathbf{z}_2 + \zeta\sigma(\mathbf{z}_0)) \tag{15}$$

where $\mathbf{n} = \mathbf{R}^\mathsf{T}[\hbar(\widehat{\mathbf{b}}_{v_1}) - \ddot{\mathbf{p}}_d + k_2\sigma(\mathbf{z}_2 + \zeta\sigma(\mathbf{z}_0)) + g\mathbf{u}_3 + \sigma(\mathbf{z}_0)]$ and $\mathbf{z}_0 = k_1(\mathbf{z}_1 + \zeta\mathbf{z}_2)$, with $\Lambda_1 = \mathrm{diag}(\lambda_{11},\, \lambda_{12},\, \lambda_{13})$, $(k_1,\, \zeta,\, \gamma_1,\, \lambda_{11},\, \lambda_{12},\, \lambda_{13}) \in \mathbb{R}^+$.

Define the angular velocity error $\mathbf{z}_3$ as

$$\mathbf{z}_3 = \Omega(\mathbf{S}(\boldsymbol{\delta})\boldsymbol{\omega} + \mathbf{n}) \tag{16}$$

whose time derivative yields

$$\begin{aligned}\dot{\mathbf{z}}_3 = {} & \delta\boldsymbol{\tau}_n\boldsymbol{\beta} + \Omega\Big[-\mathbf{S}(\boldsymbol{\omega})\mathbf{R}^\mathsf{T}(g\mathbf{u}_3 - \ddot{\mathbf{p}}_d) - \mathbf{R}^\mathsf{T}\mathbf{p}_d^{(3)} \\ & - \mathbf{S}(\boldsymbol{\omega})\mathbf{R}^\mathsf{T}\hbar(\widehat{\mathbf{b}}_{v_1}) + \mathbf{R}^\mathsf{T}\dot{\hbar}(\widehat{\mathbf{b}}_{v_1}) - \mathbf{S}(\boldsymbol{\omega})\mathbf{R}^\mathsf{T}\sigma(\mathbf{z}_0) \\ & - k_2\mathbf{S}(\boldsymbol{\omega})\mathbf{R}^\mathsf{T}\sigma(\mathbf{z}_2 + \zeta\sigma(\mathbf{z}_0)) + \boldsymbol{\alpha}_1\dot{\mathbf{z}}_2 + \boldsymbol{\alpha}_2\dot{\mathbf{z}}_0\Big]\end{aligned} \tag{17}$$

where $\Omega = [\mathbf{I}_{2\times 2},\, \mathbf{0}_{2\times 1}]$, $\boldsymbol{\tau}_n = \mathrm{diag}(\tau_2,\, \tau_1)$, $\boldsymbol{\beta} = [-J_2^{-1},\, J_1^{-1}]$,

$$\boldsymbol{\alpha}_1 = k_2\mathbf{R}^\mathsf{T}\,\mathrm{diag}\left(\frac{\partial\sigma(\mathbf{z}_2 + \zeta\sigma(\mathbf{z}_0))}{\partial(\mathbf{z}_2 + \zeta\sigma(\mathbf{z}_0))}\right)$$

$$\boldsymbol{\alpha}_2 = \left(\zeta\boldsymbol{\alpha}_1 + \mathbf{R}^{\mathsf{T}}\right)\mathrm{diag}\left(\frac{\partial\sigma(\mathbf{z}_0)}{\partial\mathbf{z}_0}\right).$$

To stabilize (17), the torque $\boldsymbol{\tau}$, estimation laws for $\hat{\dot{\boldsymbol{\beta}}}$, $\hat{\dot{\Delta}}_2$ and $\hat{\dot{\mathbf{b}}}_{v_2}$ are chosen as

$$\boldsymbol{\tau} = [\mathbf{u}_2^{\mathsf{T}}\boldsymbol{\tau}_d,\ \mathbf{u}_1^{\mathsf{T}}\boldsymbol{\tau}_d,\ 0]^{\mathsf{T}} \tag{18}$$

$$\hat{\dot{\boldsymbol{\beta}}} = \Gamma_\beta\delta\boldsymbol{\tau}_d^{\mathsf{T}}\mathbf{z}_3 \tag{19}$$

$$\hat{\dot{\Delta}}_2 = -\gamma_2\mathbf{z}_3^{\mathsf{T}}\Omega\mathbf{B}T\mathbf{R}\mathbf{u}_3 \tag{20}$$

$$\hat{\dot{\mathbf{b}}}_{v_2} = -\Lambda_2\mathbf{B}^{\mathsf{T}}\Omega^{\mathsf{T}}\mathbf{z}_3 \tag{21}$$

where $\mathbf{B} = \boldsymbol{\alpha}_1 + k_1\zeta\mathbf{R}^{\mathsf{T}}\,\mathrm{diag}(\partial\sigma(\mathbf{z}_0)/\partial\mathbf{z}_0)$ and

$$\begin{aligned}\boldsymbol{\tau}_d = -\delta^{-1}\,\mathrm{diag}\Big(\hbar^{-1}(\widehat{\beta}_1),\ \hbar^{-1}(\widehat{\beta}_2)\Big)\big(\Omega(-\mathbf{S}(\boldsymbol{\omega})\\ \times\mathbf{R}^{\mathsf{T}}(g\mathbf{u}_3 - \ddot{\mathbf{p}}_d) - \mathbf{R}^{\mathsf{T}}\mathbf{p}_d^{(3)} - \mathbf{S}(\boldsymbol{\omega})\mathbf{R}^{\mathsf{T}}\hbar(\widehat{\mathbf{b}}_{v_1})\\ + \mathbf{R}^{\mathsf{T}}\dot{\hbar}(\widehat{\mathbf{b}}_{v_1}) - \mathbf{S}(\boldsymbol{\omega})\mathbf{R}^{\mathsf{T}}\sigma(\mathbf{z}_0) + k_3\sigma(\mathbf{z}_3)\\ - k_2\mathbf{S}(\boldsymbol{\omega})\mathbf{R}^{\mathsf{T}}\sigma(\mathbf{z}_2 + \zeta\sigma(\mathbf{z}_0)) + \boldsymbol{\alpha}_1\hat{\dot{\mathbf{z}}}_2\\ + \boldsymbol{\alpha}_2\hat{\dot{\mathbf{z}}}_0 + \mathbf{R}^{\mathsf{T}}(\mathbf{z}_2 + \zeta\sigma(\mathbf{z}_0))\big)\Big)\end{aligned} \tag{22}$$

with $\hat{\dot{\mathbf{z}}}_2 = -\hat{\dot{\Delta}}_2T\mathbf{R}\mathbf{u}_3 + g\mathbf{u}_3 + \hat{\mathbf{b}}_{v_2} - \ddot{\mathbf{p}}_d$, $\hat{\dot{\mathbf{z}}}_0 = k_1(\dot{\mathbf{z}}_1 + \zeta\hat{\dot{\mathbf{z}}}_2)$, and $\Gamma_\beta = \mathrm{diag}(\gamma_{\beta_1}, \gamma_{\beta_2})$, $\Lambda_2 = \mathrm{diag}(\lambda_{21}, \lambda_{22}, \lambda_{23})$, $(\gamma_{\beta_1}, \gamma_{\beta_2}, \lambda_{21}, \lambda_{22}, \lambda_{23}, \gamma_2) \in \mathbb{R}^+$. To summarize the main result, the following theorem is given.

*Theorem 2:* By using the designed control inputs (13), (18), and the estimation laws (14), (15), (19), (20), (21), the tracking errors $\mathbf{z}_1, \mathbf{z}_2, \mathbf{z}_3$, defined in (9), (10), (16), respectively, are globally driven to the neighborhood of zero, achieving global uniformly ultimately boundedness. Meanwhile, the generated thrust force $T$, defined in (13), is bounded by a predefined positive value.

*Proof:* Defining a Lyapunov candidate function as

$$\begin{aligned}V = \frac{1}{2}\mathbf{z}_2^{\mathsf{T}}\mathbf{z}_2 + \frac{1}{k_1}\int_0^{\mathbf{z}_0}\sigma(\mathbf{s})^{\mathsf{T}}\mathbf{1}_{3\times1}d\mathbf{s} + \frac{1}{2}\mathbf{z}_3^{\mathsf{T}}\mathbf{z}_3\\ + \sum_{i=1}^{2}\gamma_i^{-1}\int_0^{\widetilde{\Delta}_i}(\hbar(\rho+\Delta) - \Delta)d\rho\\ + \sum_{i=1}^{3}\lambda_{1i}^{-1}\int_0^{\widetilde{b}_{v_{1i}}}\big(\hbar(\rho + b_{v_i}) - b_{v_i}\big)d\rho\\ + \sum_{i=1}^{3}\lambda_{2i}^{-1}\int_0^{\widetilde{b}_{v_{2i}}}\big(\hbar(\rho + b_{v_i}) - b_{v_i}\big)d\rho\\ + \sum_{i=1}^{2}\gamma_{\beta_i}^{-1}\int_0^{\widetilde{\beta}_i}(\hbar(\rho+\beta_i) - \beta_i)d\rho\end{aligned}$$

where $\widetilde{\Delta}_1 = \widehat{\Delta}_1 - \Delta$, $\widetilde{\Delta}_2 = \widehat{\Delta}_2 - \Delta$, $\widetilde{\mathbf{b}}_{v_1} = \widehat{\mathbf{b}}_{v_1} - \mathbf{b}_v$, $\widetilde{\mathbf{b}}_{v_2} = \widehat{\mathbf{b}}_{v_2} - \mathbf{b}_v$, $\widetilde{\boldsymbol{\beta}} = \widehat{\boldsymbol{\beta}} - \boldsymbol{\beta}$ denote estimation errors. Computing the time derivative of $V$ and substituting (13), (14), (15), (18), (19), (20), (21) into $\dot{V}$, in closed-loop, we obtain

$$\begin{aligned}\dot{V} = -k_2(\mathbf{z}_2 + \zeta\sigma(\mathbf{z}_0))^{\mathsf{T}}\sigma(\mathbf{z}_2 + \zeta\sigma(\mathbf{z}_0))\\ - \zeta\sigma(\mathbf{z}_0)^{\mathsf{T}}\sigma(\mathbf{z}_0) - k_3\mathbf{z}_3^{\mathsf{T}}\sigma(\mathbf{z}_3) + \sigma(\mathbf{z}_0)^{\mathsf{T}}\mathbf{R}\boldsymbol{\delta}.\end{aligned} \tag{23}$$

By using the Young's inequality, we have

$$\sigma(\mathbf{z}_0)^{\mathsf{T}}\mathbf{R}\boldsymbol{\delta} \le \frac{1}{4\epsilon}\|\sigma(\mathbf{z}_0)\|^2 + \epsilon\delta^2 \tag{24}$$

with $\epsilon \in \mathbb{R}^+$. Substituting (24) into (23), $\dot{V}$ becomes,

$$\begin{aligned}\dot{V} \le -k_2(\mathbf{z}_2 + \zeta\sigma(\mathbf{z}_0))^{\mathsf{T}}\sigma(\mathbf{z}_2 + \zeta\sigma(\mathbf{z}_0))\\ - (\zeta - 1/(4\epsilon))\|\sigma(\mathbf{z}_0)\|^2\\ - k_3\mathbf{z}_3^{\mathsf{T}}\sigma(\mathbf{z}_3) + \epsilon\delta^2\end{aligned}$$

where $\zeta$, $\epsilon$ are chosen properly such that $\zeta > 1/(4\epsilon)$ holds. For convenience and clarity, we set $\kappa_1 = \zeta - 1/(4\epsilon)$, $\kappa_2 = k_2$, $\kappa_3 = k_3$, $\delta_n = \epsilon\delta^2$, leading to a new expression for $\dot{V}$, given by

$$\begin{aligned}\dot{V} \le -\kappa_1\|\sigma(\mathbf{z}_0)\|^2 - \kappa_2(\mathbf{z}_2 + \zeta\sigma(\mathbf{z}_0))^{\mathsf{T}}\\ \times\sigma(\mathbf{z}_2 + \zeta\sigma(\mathbf{z}_0)) - \kappa_3\mathbf{z}_3^{\mathsf{T}}\sigma(\mathbf{z}_3) + \delta_n\end{aligned} \tag{25}$$

with $(\kappa_1, \kappa_2, \kappa_3, \delta_n) \in \mathbb{R}^+$. From (25), we can further get the following inequalities

$$\dot{V} \le -\kappa_1\sigma(\|\mathbf{z}_0\|)^2 + \delta_n,\ \dot{V} \le -\kappa_3\|\mathbf{z}_3\|\sigma(\|\mathbf{z}_3\|) + \delta_n$$
$$\dot{V} \le -\kappa_2\|\mathbf{z}_2 + \zeta\sigma(\mathbf{z}_0)\|\sigma(\|\mathbf{z}_2 + \zeta\sigma(\mathbf{z}_0)\|) + \delta_n$$

from which we can conclude that $\|\mathbf{z}_0\|$, $\|\mathbf{z}_3\|$, $\|\mathbf{z}_2 + \zeta\sigma(\mathbf{z}_0)\|$ are ultimately bounded by $\bar{z}_0 = \sigma^{-1}(\sqrt{\delta_n/\kappa_1}) + \epsilon_n$, $\bar{z}_3 = \vartheta^{-1}(\delta_n/\kappa_3) + \epsilon_n$, $\bar{z}_{20} = \vartheta^{-1}(\delta_n/\kappa_2) + \epsilon_n$, respectively, which can be made arbitrarily small by increasing $\kappa_1$, $\kappa_2$, $\kappa_3$, with $\vartheta(z) = z\sigma(z)$, $z \ge 0$, $\sigma_{\max} > \bar{z}_0$, $\epsilon_n \in \mathbb{R}^+$.

In addition, we have $\|\mathbf{z}_2 + \zeta\sigma(\mathbf{z}_0)\| \ge |\|\mathbf{z}_2\| - \zeta\|\sigma(\mathbf{z}_0)\||$, resulting in

$$\|\mathbf{z}_2\| \le \|\mathbf{z}_2 + \zeta\sigma(\mathbf{z}_0)\| + \zeta\|\sigma(\mathbf{z}_0)\|. \tag{26}$$

As we established before,

$$\lim_{t\to\infty}\|\sigma(\mathbf{z}_0)\| \le \bar{z}_0,\ \lim_{t\to\infty}\|\mathbf{z}_2 + \zeta\sigma(\mathbf{z}_0)\| \le \bar{z}_{20}. \tag{27}$$

Combing (26) and (27), we obtain

$$\lim_{t\to\infty}\|\mathbf{z}_2\| \le \bar{z}_{20} + \zeta\bar{z}_0 + \epsilon_n,$$

from which we conclude that $\|\mathbf{z}_2\|$ is ultimately bounded by $\bar{z}_2 = \bar{z}_{20} + \zeta\bar{z}_0 + \epsilon_n$.

Going back to $\mathbf{z}_0$, we have $\|\mathbf{z}_0\| \ge k_1|\|\mathbf{z}_1\| - \zeta\|\mathbf{z}_2\||$ leading to $\|\mathbf{z}_1\| \le k_1^{-1}\|\mathbf{z}_0\| + \zeta\|\mathbf{z}_2\|$ and, further

$$\lim_{t\to\infty}\|\mathbf{z}_1\| \le \bar{z}_0/k_1 + \zeta\bar{z}_2 + \epsilon_n.$$

Consequently, $\|\mathbf{z}_1\|$ is ultimately bounded by $\bar{z}_1 = \bar{z}_0/k_1 + \zeta\bar{z}_2 + \epsilon_n$. At last, we prove the designed thrust force is always bounded by a predefined value. From (13), we have

$$T \le m_{\max}\big(\|g\mathbf{u}_3 - \ddot{\mathbf{p}}_d\|_\infty + \bar{b}_v + k_2\sigma_{\max} + \sigma_{\max}\big). \tag{28}$$

The proof is done. ■

*Remark 4:* The designed $\boldsymbol{\tau}_d$, defined in (22), is always well-defined since $\delta$, $\hbar(\widehat{\beta}_1)$, $\hbar(\widehat{\beta}_2)$ are nonzero.

*Remark 5:* The quadrotor aerial vehicle, whose kinematics and dynamics are described by (1)-(2), is an underactuated vehicle. Due to their underactuated nature quadrotors do not satisfy the Brockett's necessary condition for the existence of smooth time-invariant feedback controllers. In addition, a naive backstepping implementation could cause singularities in the control inputs. To solve this problem, we introduce a constant vector $\boldsymbol{\delta}$ as in (10). Similar analysis can also be found in [26].

*Remark 6:* From the analysis above, we conclude that to reduce the upper bound of the position error, theoretically, we should increase the values of control gains $k_1$, $k_2$, $k_3$ and

decrease $\delta$. However, they cannot be any large/small values, e.g., too large $k_3$ or too small $\delta$ could lead to undesirable oscillation since the designed torque is proportional to $k_3$ and $\delta^{-1}$. With respect to the role of estimation gains, e.g., $\lambda_{11}, \lambda_{12}, \ldots, \gamma_1, \gamma_2$, if they are chosen to be too large, the updating rate will be too fast, leading to undesirable overshoot. Therefore, we need to find a trade-off between the tracking accuracy (updating rate) and the magnitude of the oscillation (overshoot).

*Remark 7:* From Theorem 2, we can conclude that the error terms, $\mathbf{z}_1$, $\mathbf{z}_2$, $\mathbf{z}_3$, converge globally to the neighborhood of zero, regardless of uncertain parameters and external disturbances, which are compensated by the integrators embedded in the designed control inputs, $T$ and $\boldsymbol{\tau}$, which is very useful for dynamic systems that are difficult to identify precisely.

## V. Simulation Validation

To demonstrate the performance of the proposed control strategy, simulation results are presented and discussed in this section. Moreover, we also provide a comparison with existing results to illustrate the enhanced performance by using the proposed control strategy. The main parameters used for the simulation are chosen as: $k_1 = 5$, $k_2 = 3$, $k_3 = 4$, $\zeta = 0.5$, $\gamma_1 = 0.8$, $\gamma_2 = 0.01$, $\Lambda_1 = \text{diag}(0.01, 0.01, 0.01)$, $\Lambda_2 = \text{diag}(0.01, 0.01, 0.01)$, $\Gamma_\beta = \text{diag}(0.01, 0.01)$, $m = 0.2\,(\text{kg})$, $\mathbf{J} = \text{diag}(6.5, 6.5, 13.0) \cdot 10^{-4}(\text{kg}\cdot\text{m}^2)$, $\mathbf{b}_v = [0.1, 0.2, 0.3]^{\mathsf{T}}\,(\text{m}\cdot\text{s}^{-2})$, and the saturation function $\sigma(\cdot) = \sigma_{\max}\tanh(\cdot)$, $\sigma_{\max} = 1.5$. The smooth reference trajectory $\mathbf{p}_d(t)$ is selected as

$$\mathbf{p}_d(t) = \mathbf{R}_x(\pi/20)\begin{bmatrix} a_x \sin(w_x t + \pi/2) \\ a_y \sin(w_y t) \\ a_z \end{bmatrix} (\text{m})$$

which is a Lissajous curve, with $a_x = 2.0$, $a_y = 2.0$, $a_z = -1.5$. To generate different desired linear velocities for the quadrotor, the sets for $w_x$, $w_y$ are chosen as: i) $w_x = 0.3\,(\text{rad/s})$, $w_y = 0.2\,(\text{rad/s})$; ii) $w_x = 0.9\,(\text{rad/s})$, $w_y = 0.6\,(\text{rad/s})$. Figure 1 displays the desired trajectory and the quadrotor's actual trajectory, together with Figure 2, we can conclude that the vehicle eventually tracks closely the desired trajectory. From Figure 2, we can also conclude that the designed controller is able to drive the quadrotor to track a more aggressive trajectory ($w_x = 0.9\,(\text{rad/s})$, $w_y = 0.6\,(\text{rad/s})$) with almost the same position error as the result obtained from tracking a slower trajectory ($w_x = 0.3\,(\text{rad/s})$, $w_y = 0.2\,(\text{rad/s})$), in steady state. In addition, Figure 3 depicts the time evolution of the thrust force $T$, showing that for different desired linear velocities, the thrust force $T$ is always bounded by its corresponding theoretical upper bound $T_{\max_1} = 5.04\,(\text{N})$ and $T_{\max_1} = 5.16\,(\text{N})$, respectively, calculated through (28), where $m_{\max} = 0.3\,(\text{kg})$, $\bar{b}_v = 1.0\,(\text{m}\cdot\text{s}^{-2})$.

As the proposed control laws do not dependent on the exact mass and inertia of the quadrotor, the same control law with the same parameters and gains can be used for i) cargo transportation; ii) controlling a wide range of vehicles, having different masses and inertia moments without loss of performance. To highlight this distinctive feature, for $w_x = 0.3\,(\text{rad/s})$, $w_y = 0.2\,(\text{rad/s})$, we compare the performance of

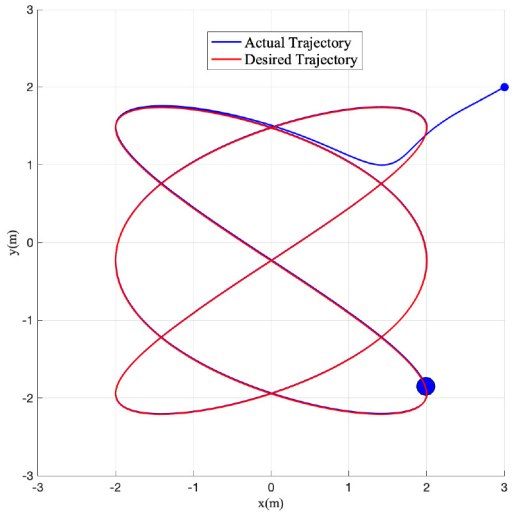


Fig. 1. Time evolution of the actual and desired trajectories seen from the above, where $w_x = 0.3\,(\text{rad/s})$, $w_y = 0.2\,(\text{rad/s})$.

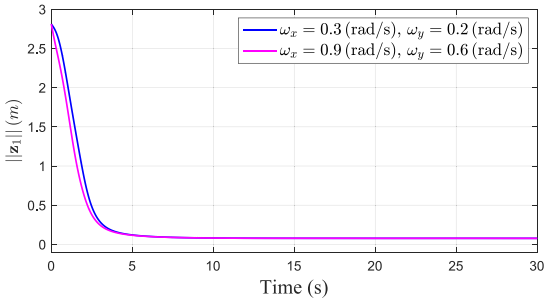


Fig. 2. Time evolution of the position error $||\mathbf{z}_1||$ with different desired linear velocities, showing that it converges to a small neighborhood of zero.

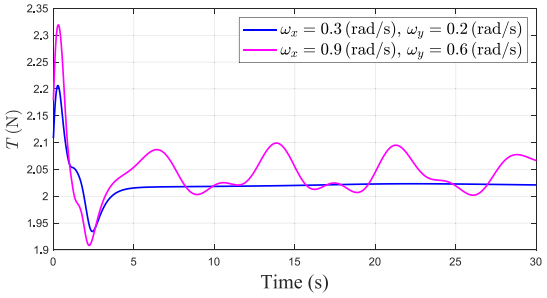


Fig. 3. Time evolution of the thrust force with different desired linear velocities.

the proposed controller with a backstepping-based nonlinear saturated tracking controller reported in [10]. This simulation is separated into three phases: 1) before $t_1 = 20\,(\text{s})$, the vehicle is controlled using the known exact mass $m = 0.2\,(\text{kg})$ as for the controller in [10], and the unknown mass with the initial estimate $\widehat{m}(0) = 0.15\,(\text{kg})$ for the controller proposed herein; 2) at $t_1 = 20\,(\text{s})$, and 3) $t_2 = 40\,(\text{s})$, the mass of the vehicle changes suddenly, mimicking the collection of loads. Figures 4 and 5 display the simulation results obtained from the method presented in [10] and the control method proposed herein, respectively. From Figure 4, we can conclude that the position error $\|\mathbf{z}_1\|$ diverges once the mass changes from 0.25 (kg)

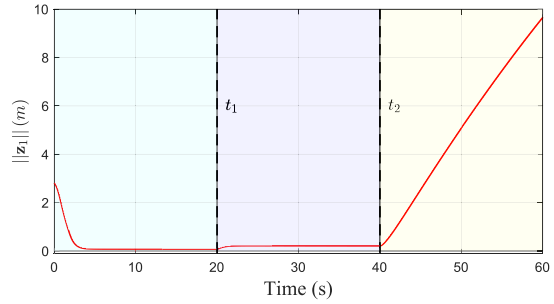


Fig. 4. Time evolution of $\|\mathbf{z}_1\|$ obtained with the method reported in [10].

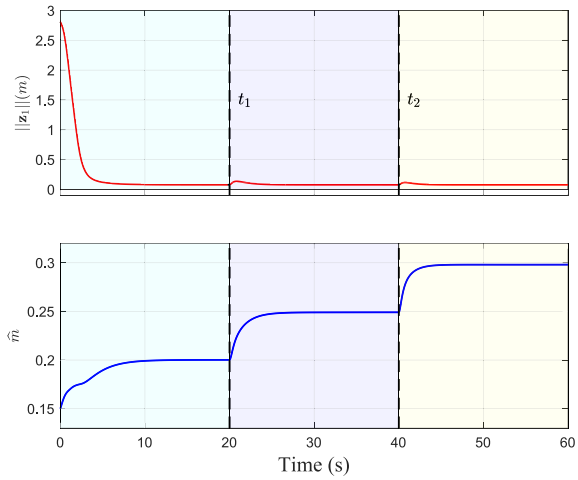


Fig. 5. Time evolution of $\|\mathbf{z}_1\|$ and $\widehat{m}$ obtained with the proposed method.

to 0.30 (kg) due to the fact that the controller in [10] cannot update the quadrotor's mass automatically. However, from Figure 5, we can conclude that the proposed controller can stabilize the quadcopter when the mass changes from 0.2 (kg) to 0.25 (kg) and from 0.25 (kg) to 0.30 (kg) because that mass estimators that can successfully compensate for the sudden changes in the vehicle's mass.

## VI. Conclusion

This letter proposed a solution to the trajectory tracking control problem with application to an underactuated quadrotor, guaranteeing that the vehicle was able to track its desired trajectory with arbitrarily small position error. To deal with the effect of uncertain system mass, moment of inertial and external disturbances, estimation laws for them were designed and incorporated into the control inputs, attaining robust adaptive performance. Saturation functions were introduced in the control laws to ensure that the designed thrust force is always bounded. In order to demonstrate the performance of the developed control strategy, simulation results were given and analyzed.

## References

[1] D. Floreano and R. J. Wood, "Science, technology and the future of small autonomous drones," *Nature*, vol. 521, pp. 460–466, May 2015.

[2] T. Lee, "Geometric control of quadrotor UAVs transporting a cable-suspended rigid body," *IEEE Trans. Control Syst. Technol.*, vol. 26, no. 1, pp. 255–264, Jan. 2018.

[3] X. Liang, Y. Fang, N. Sun, and H. Lin, "A novel energy-coupling-based hierarchical control approach for unmanned quadrotor transportation systems," *IEEE/ASME Trans. Mechatronics*, vol. 24, no. 1, pp. 248–259, Feb. 2019.

[4] K. B. Kidambi, C. Fermüller, Y. Aloimonos, and H. Xu, "Robust nonlinear control-based trajectory tracking for quadrotors under uncertainty," *IEEE Contr. Syst. Lett.*, vol. 5, no. 6, pp. 2042–2047, Dec. 2021.

[5] G. Hoffmann, S. Waslander, and C. Tomlin, "Quadrotor helicopter trajectory tracking control," in *Proc. AIAA Guid. Navig. Control Conf. Exhibit*, 2008, pp. 1–14.

[6] H. Xie, D. Cabecinhas, R. Cunha, C. Silvestre, and Q. Xu, "A trajectory tracking LQR controller for a quadrotor: Design and experimental evaluation," in *Proc. IEEE TENCON*, 2015, pp. 1–7.

[7] M. Bisheban and T. Lee, "Geometric adaptive control for a quadrotor UAV with wind disturbance rejection," in *Proc. IEEE Conf. Decis. Control*, Miami, FL, USA, 2018, pp. 2816–2821.

[8] M. Bisheban and T. Lee, "Geometric adaptive control with neural networks for a quadrotor in wind fields," *IEEE Trans. Control Syst. Technol.*, vol. 29, no. 4, pp. 1533–1548, Jul. 2021.

[9] H. Hua, Y. Fang, X. Zhang, and B. Lu, "A novel robust observer-based nonlinear trajectory tracking control strategy for quadrotors," *IEEE Trans. Control Syst. Technol.*, vol. 29, no. 5, pp. 1952–1963, Sep. 2021.

[10] W. Xie, G. Yu, D. Cabecinhas, R. Cunha, and C. Silvestre, "Global saturated tracking control of a quadcopter with experimental validation," *IEEE Contr. Syst. Lett.*, vol. 5, no. 1, pp. 169–174, Jan. 2021.

[11] G. Yu, D. Cabecinhas, R. Cunha, and C. Silvestre, "Quadrotor trajectory generation and tracking for aggressive maneuvers with attitude constraints," *IFAC-PapersOnLine*, vol. 52, no. 12, pp. 55–60, 2019.

[12] Q. Lu, B. Ren, and S. Parameswaran, "Uncertainty and disturbance estimator-based global trajectory tracking control for a quadrotor," *IEEE/ASME Trans. Mechatronics*, vol. 25, no. 3, pp. 1519–1530, Jun. 2020.

[13] H. Ríos, R. Falcón, O. A. González, and A. Dzul, "Continuous sliding-mode control strategies for quadrotor robust tracking: Real-time application," *IEEE Trans. Ind. Electron.*, vol. 66, no. 2, pp. 1264–1272, Feb. 2019.

[14] L.-X. Xu, H.-J. Ma, D. Guo, A.-H. Xie, and D.-L. Song, "Backstepping sliding-mode and cascade active disturbance rejection control for a quadrotor UAV," *IEEE/ASME Trans. Mechatronics*, vol. 25, no. 6, pp. 2743–2753, Dec. 2020.

[15] H. Castañeda and J. L. Gordillo, "Spatial modeling and robust flight control based on adaptive sliding mode approach for a quadrotor MAV," *J. Intell. Robot. Syst.*, vol. 93, pp. 101–111, Feb. 2019.

[16] H. Castañeda, J. Rodriguez, and J. L. Gordillo, "Continuous and smooth differentiator based on adaptive sliding mode control for a quadrotor MAV," *Asian J. Control*, vol. 23, no. 2, pp. 661–672, 2021.

[17] L. Yu, G. He, X. Wang, and L. Shen, "A novel fixed-time sliding mode control of quadrotor with experiments and comparisons," *IEEE Contr. Syst. Lett.*, vol. 6, pp. 770–775, 2022.

[18] D. Wang, Q. Pan, Y. Shi, J. Hu, and C. Zhao, "Efficient nonlinear model predictive control for quadrotor trajectory tracking: Algorithms and experiment," *IEEE Trans. Cybern.*, vol. 51, no. 10, pp. 5057–5068, Oct. 2021.

[19] S. C. Yogi, V. K. Tripathi, and L. Behera, "Adaptive integral sliding mode control using fully connected recurrent neural network for position and attitude control of quadrotor," *IEEE Trans. Neural Netw. Learn. Syst.*, early access, Apr. 21, 2021, doi: 10.1109/TNNLS.2021.3071020.

[20] F. Jiang, F. Pourpanah, and Q. Hao, "Design, implementation, and evaluation of a neural-network-based quadcopter UAV system," *IEEE Trans. Ind. Electron.*, vol. 67, no. 3, pp. 2076–2085, Mar. 2020.

[21] X. Zhang *et al.*, "Compound adaptive fuzzy quantized control for quadrotor and its experimental verification," *IEEE Trans. Cybern.*, vol. 51, no. 3, pp. 1121–1133, Mar. 2021.

[22] F. Santoso, M. A. Garratt, and S. G. Anavatti, "Hybrid PD-fuzzy and PD controllers for trajectory tracking of a quadrotor unmanned aerial vehicle: Autopilot designs and real-time flight tests," *IEEE Trans. Syst., Man, Cybern., Syst.*, vol. 51, no. 3, pp. 1817–1829, Mar. 2021.

[23] Y. Zou and Z. Meng, "Immersion and invariance-based adaptive controller for quadrotor systems," *IEEE Trans. Syst., Man, Cybern., Syst.*, vol. 49, no. 11, pp. 2288–2297, Nov. 2019.

[24] A. R. Teel, "Adaptive tracking with robust stability," in *Proc. 32nd IEEE Conf. Decis. Control*, San Antonio, TX, USA, 1993, pp. 570–575.

[25] B. Yao and M. Tomizuka, "Adaptive robust control of SISO nonlinear systems in a semi-strict feedback form," *Automatica*, vol. 33, no. 5, pp. 893–900, 1997.

[26] A. P. Aguiar and J. P. Hespanha, "Trajectory-tracking and path-following of underactuated autonomous vehicles with parametric modeling uncertainty," *IEEE Trans. Autom. Control*, vol. 52, no. 8, pp. 1362–1379, Aug. 2007.